

Primljen / Received: 19.6.2017.

Ispravljen / Corrected: 5.4.2018.

Prihvaćen / Accepted: 22.10.2018.

Dostupno online / Available online: 10.3.2019.

Evaluation of frost blanket layer strength using different devices

Authors:



Assoc.Prof. **Lina Bertulienė**, PhD. CE
Vilnius Gediminas Technical University, Lithuania
Department of Roads
lina.bertuliene@vgtu.lt



Assoc.Prof. **Lina Juknevičiūtė-Žilinskienė**, PhD. CE
Vilnius Gediminas Technical University, Lithuania
Department of Roads
lina.juknevičiute-zilinskiene@vgtu.lt



Prof. **Henrikas Sivilevičius**, PhD. CE
Vilnius Gediminas Technical University, Lithuania
Department of Mobile Machinery
and Railway Transport
henrikas.sivilevicius@vgtu.lt



Prof. **Alfredas Laurinavičius**, PhD. CE
Vilnius Gediminas Technical University, Lithuania
Department of Roads
alfredas.laurinavicius@vgtu.lt

Preliminary note

Lina Bertulienė, Lina Juknevičiūtė-Žilinskienė, Henrikas Sivilevičius, Alfredas Laurinavičius

Evaluation of frost blanket layer strength using different devices

The relationship between the static and dynamic deflection modulus is presented in the paper, and a correlation between the FBL physical and strength indicators is determined. The correction coefficients of dynamic measurements, as related to static beam readings, are presented. The results show that, in the absence of a static beam, static beam readings can be replaced by the readings of any of the three analysed dynamic devices, and the FBL strength can thus be measured.

Key words:

pavement structure, frost blanket layer, deflection modulus, coefficient of filtration

Prethodno priopćenje

Lina Bertulienė, Lina Juknevičiūtė-Žilinskienė, Henrikas Sivilevičius, Alfredas Laurinavičius

Ocjena nosivosti sloja kolničke konstrukcije za zaštitu od smrzavanja primjenom različitih mjernih uređaja

U ovom radu prikazan je odnos između statičkog i dinamičkog deformacijskog modula, te je uspostavljena korelacija između fizičkih svojstava i pokazatelja nosivosti sloja kolničke konstrukcije za zaštitu od smrzavanja. Prikazani su korekcijski koeficijenti dinamičkih mjerenja u odnosu na statička očitavanja. Rezultati pokazuju da u odsutnosti statičkog mjernog uređaja mogu se statička očitavanja zamijeniti očitanjima bilo kojih od tri predstavljene vrste dinamičkih uređaja, te na taj način odrediti nosivost sloja kolničke konstrukcije za zaštitu od smrzavanja.

Ključne riječi:

kolnička konstrukcija, sloj za zaštitu od smrzavanja, deformacijski modul, koeficijent filtracije

Vorherige Mitteilung

Lina Bertulienė, Lina Juknevičiūtė-Žilinskienė, Henrikas Sivilevičius, Alfredas Laurinavičius

Bewertung der Tragfähigkeit der Frostschuttschicht der Fahrbahnkonstruktion durch Anwendung verschiedener Messgeräte

In dieser Abhandlung wird die Beziehung zwischen dem statischen und dem dynamischen Verformungsmodul dargestellt, und es wurde eine Korrelation zwischen den physischen Eigenschaften und den Indikatoren der Tragfähigkeit der Frostschuttschicht der Fahrbahnkonstruktion hergestellt. Dargestellt werden die Korrelationskoeffizienten der dynamischen Messungen im Vergleich zu den statischen Messwerten. Die Ergebnisse zeigen, dass beim Fehlen eines statischen Messgerätes das statische Ablesen durch das Ablesen irgendeines der drei vorgestellten dynamischen Geräte ersetzt werden kann, und man kann auf diese Weise die Tragfähigkeit der Frostschuttschicht der Fahrbahnkonstruktion bestimmen.

Schlüsselwörter:

Fahrbahnkonstruktion, Frostschuttschicht, Verformungsmodul, Filtrationskoeffizient

1. Introduction

A protective frost blanket layer (FBL) of road pavement structures is strictly necessary in the climate zones where high air temperature variations and moisture are prevalent. The layer has to withstand the load of traffic, pavement and base layers, and transmit such load to the subgrade soil. Besides, the layer drains pavement base and compensates for surface irregularities during installation. The main purpose of this layer is to protect pavement structure from damaging effects of frost. The FBL consists of non-frost-susceptible soils or unbound mineral mixtures, which have to be watertight and capable of preventing capillary rise of water to the base layer even after their compaction.

The three elements necessary for formation of ice lenses and thus for frost heave are the frost susceptible soil, subfreezing temperatures, and water (must be available from the shallow groundwater table, infiltration, an aquifer, or must be present in voids of fine-grained soil). Unfortunately, all three conditions are met in many northern regions [1]. Ice crystals form when water freezes in layers above the FBL, and water can be attracted to the area with freezing temperatures. Then this water freezes further, attracting more and more water from the next layer and thus the thickness of ice layer increases. A negative impact on the road structure occurs during thawing [2-4]. The FBL is formed of coarse materials (sand, gravel, sand-gravel and gravel-sand mixtures), and it forms large-size intergranular space channels [5] that prevent formation of capillaries. The FBL model of the water flow regime is shown in Figure 1.

The infiltration water from upper pavement layers can drain through transverse slope to the shoulder, and filter into the FBL.

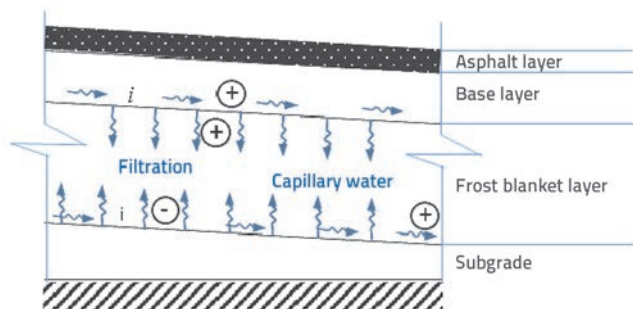


Figure 1. Impact of water flow regime on road structure ("+" – positive effect of water, "-" – negative effect of water)

A capillary barrier is a layer of coarse-grained soils or geosynthetic material in a frost-susceptible soil, which reduces the upward capillary flow of soil water due to suction gradient generated by evaporation or freezing, and reduces or prevents water from infiltrating from the overlying fine-pored unsaturated soil into the soil below the

capillary barrier. Granular capillary barriers have been used successfully to reduce frost heaving of roads [1]. A properly installed drainage reduces road maintenance operating costs and extends service life of roads [6].

The static plate loading test is used in many European countries [7] for assessing quality of earthworks. The deflection modulus is the result of the test and there are limitations set by local standards for achieving minimum value of the modulus. For example, in Germany, Austria, and Czech Republic, the measurement of deflection modulus, obtained from the second loading cycle, is one of the essential tests to be conducted before laying pavement layers.

The load exerted by vehicle wheels on pavement structure is one of the most important factors that determine behaviour of road surface during its life-cycle. In order to optimally use resources available for road construction [8, 9], it is imperative to collect the information about the properties of materials to be used, and about their interaction [10-14].

Vennapusa et al. [15] presented experimental tests comparing the in situ measurements by means of the falling weight deflectometer (FWD), light weight deflectometer (LWD), dynamic cone penetrometer, and static piezocone.

Various falling weight deflectometers [16] are used to determine structural strength of pavements. During the pavement construction stage, the LWD-type devices can be used to determine deflection modulus of non-binder pavement layers [17]. The stiffness modulus and the density of road subgrade contribute significantly to the long-term performance of pavement structures. Chai et al. [18] presented a case study in which the FWD test was used to evaluate whether the subgrade layer achieved the required design stiffness modulus and density during construction.

The static and dynamic deflection measurement methods are used to determine deflection modulus of pavements. During static deflection measurements, an area of the road pavement structure is gradually loaded and unloaded. The essence of evaluating structural strength of roads is to add certain pressure to the road surface which, according to the definition, corresponds to the load impact of vehicle wheels at the pressure point. The disadvantage of the static method is that, at present, it is not possible to determine the road structure's capability to transfer dynamic effects that occur due to real vehicle traffic. Dynamic methods accurately reflect the impact of forces affecting the road structure. This is made possible because the vehicle wheel load is transmitted to the road when the vehicle actually moves along the road.

The aim of this research is to compare static and dynamic methods used for measuring the FBL, and to determine whether dynamic methods are more effective, and whether they could actually replace static methods.

The interaction between physical FBL indicators and the FBL deflection modulus, measured by static and dynamic devices, is determined in the paper. The correction coefficients,

obtained by means of statistical analyses, enable replacement of the readings of dynamic devices by the static beam (SB) readings.

2. Analysis of static and dynamic deflection modulus

Dependencies between dynamic and static deflection moduli are rarely used in practice. Most commonly, the limit values are given for both the static and dynamic moduli E_{v_2} and E_{v_d} , respectively. Based on the currently valid Construction Rules of Lithuania, deflection modulus values for the layers of loose materials are specified according to the compaction degree of the layer [19].

According to Bilodeau & Doré [20, 21] in FWD tests, the dynamic force $F(N)$ is applied to the tested surface through the potential energy of a mass suspended at a given height $h(m)$. The dynamic force is determined with eq. (1) [22]:

$$F = m \cdot h \cdot g \quad (1)$$

where: m is the mass (kg), and g is the gravitational acceleration (ms^{-2}). Knowing the loading plate radius a , the stress σ_0 directly under the plate is determined by eq. (2):

$$\sigma_0 = \frac{F}{\pi a^2} \quad (2)$$

for which a uniform distribution is generally assumed. For FWD tests, the surface elastic modulus can be obtained from the solution of Boussinesq Equations [23] using the measured surface deflection d_0 at the centre of a rigid loading plate. For a semi-infinite space, the surface elastic modulus E is expressed by eq. (3):

$$E = \frac{f \sigma_0 a (1 - \nu^2)}{d_0} \quad (3)$$

where ν is the Poisson ratio, and f is the correction factor (stress distribution factor) dependent on stress distribution. As f is 2 for a uniform stress distribution under the loading plate, Ullidtz [23] suggested that the theoretical stress distribution under a rigid plate resting on an elastic material assumes infinite values at the plate edges.

Kavussi et al. [24] examined how the portable Falling Weight Deflectometer (PFWD) is used to determine the pavement deflection modulus. The results of experimental studies showed that there is a good correlation between PFWD and FWD.

Tompai [25] conducted a comparative analysis of the static method (B & C Small – Plate Device) and dynamic method (light falling weight deflectometer, LFWD). The possibility of reliable conversion between the values of two dynamic moduli (E_{v_d} , E_d) obtained by using the LFWD and the static

modulus E_2 is briefly presented and justified. The new dynamic target values could open up the opportunity to perform the quality control and to assess bearing strength of the tested layer not only by the static plate load test, which proved to be time-consuming and labour intensive, but also by dynamic devices.

The first research results based on the use of the Light Falling Weight Deflectometer ZFG 01 were published by Sulewska in [26]. She established functional dependencies between the dynamic and static deformation moduli $E_d = f(I_s)$, $E_d = f(E_1)$, $E_d = f(E_2)$ (where E_d - dynamic modulus of soil deformation, E_1 and E_2 - primary and secondary moduli of soil deformation, I_s - value of soil degree of compaction). The author concluded that the LFWD can be used as a control measure to determine the deformation modulus of sand-gravel layers. In further studies, Sulewska [27] examined the soil compaction degree for embankments using the LFWD. The objective of this study was to find a correlation between the deflection modulus, measured by the Falling Weight Deflectometer ZFG 02, and the compaction rate.

According to the authors of [28, 29], it can be assumed that there is a certain interaction between the measurement data obtained by static and dynamic devices. A theoretical model for the comparison of static and dynamic device readings, with three possible cases, is presented in Figure 2. In the first case, the static and dynamic device readings are the same, and regression line runs at an angle of 45° . In the second case, the dynamic device readings are higher than those of the static device. In the third case, the dynamic device readings are lower than those of the static device.

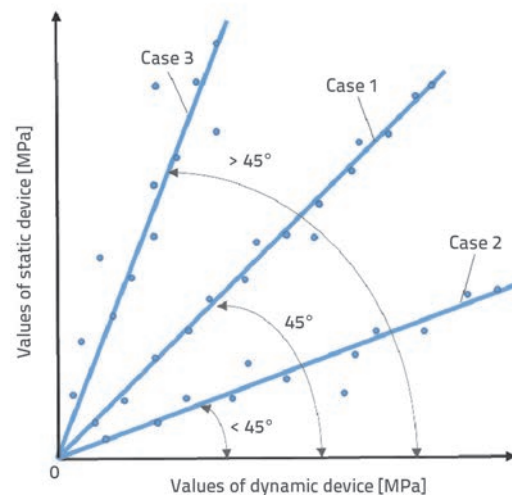


Figure 2. Correlation models of static and dynamic device readings (Case 1: both readings are almost the same; Case 2: static device readings are lower than dynamic device readings; Case 3: static device readings exceed dynamic device readings)

In Lithuania, approximate values of dynamic deflection modulus E_{vd} correction to the static deflection modulus E_{v2} are given in LST 1360.5:1995 [30], where E_{v2} – static deflection modulus, E_{vd} – dynamic deflection modulus.

Figure 3 shows that the dependency between the values of dynamic and static deflection moduli is linear. The higher the dynamic modulus E_{vd} value, the higher the static modulus E_{v2} value. In normative documents, the graph corresponds to the third line of the theoretical model (Figure 2). The graph (Figure 3) does not specify to which dynamic device it corresponds. It is likely that the correlation between the readings of each dynamic device and static device is different. Dynamic methods can be successfully applied as an alternative to the static method.

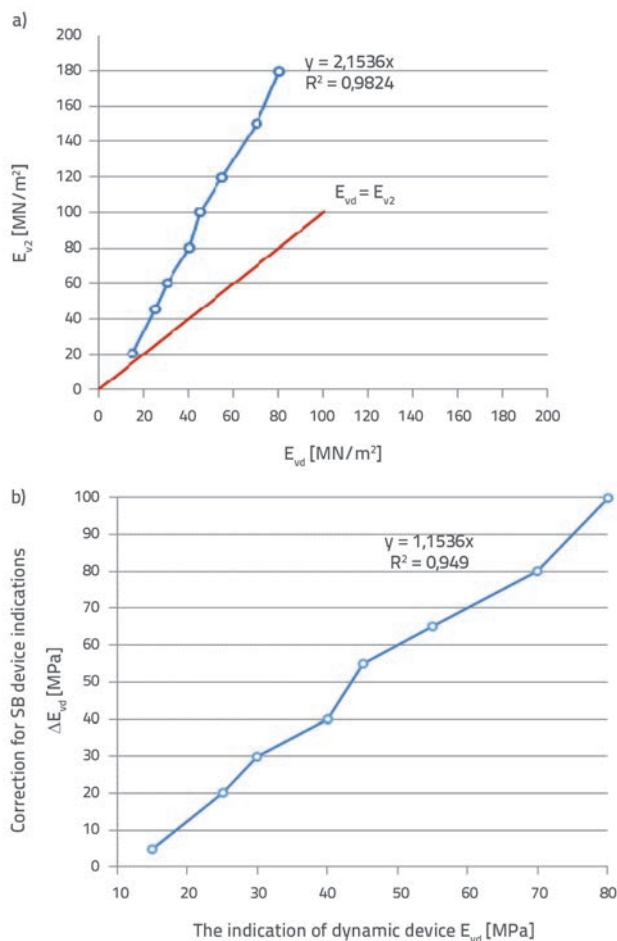


Figure 3. Dependencies of dynamic deflection modulus E_{vd} correction to static deflection modulus E_{v2} : a) absolute values; b) added correction values

3. Experimental design

The following experimental research had to be carried out in order to theoretically justify the suitability of static and dynamic measuring methods, and the compatibility of measuring devices for measuring the FBL strength:

- Static and dynamic methods were used to measure deflection moduli under field conditions

- Physical indicators were determined in laboratory, and their impact on deflection moduli was measured from regression equations
- The interaction between the readings of dynamic devices and SB was determined
- Average coefficients for the correction of readings of each dynamic device into SB readings were calculated.

A 710 m long test section for special experimental pavement structures was constructed in an open area in Vilnius region, Lithuania [31]. It has no horizontal curves in plan and vertical curves in longitudinal profile, and is characterized by the same draining conditions along the entire length. The cross-section parameters of the test section correspond to the 3rd category of roads, and the pavement structure corresponds to the 3rd class of pavement structures in accordance with the Standardized Design Rules for Road Pavement Structures [32]. The test section was constructed in the following stages:

- The existing asphalt pavement was milled down to the base layer made of loose materials
- Pavement base layers were dug out to the design subgrade level
- Deflection modulus values, higher than normative ones, were achieved during reconstruction of subgrade and installation of FBL [33]. The subgrade compaction values varied between 95-100% and the deflection modulus of the top layer amounted to no less than 45 MPa. Similarly, based on the same standards, the FBL compaction values varied between 100 and 103%. In case of SV (the highest class) and I to IV class pavement structures, the value of FBL deflection modulus had to be at least 120 MPa, while in class V and VI pavement structures these values had to be no less than 100 MPa and 80 MPa.

The 710 m test section consisted of 26 sub-sections each measuring 30 m in length, and one sub-section 20 m in length (Figure 4). The test section represented 5 different road pavement structures (in other road pavement structures the base layers and upper asphalt layers are different; these other structures are not presented in this paper as it concentrates on FBL only).

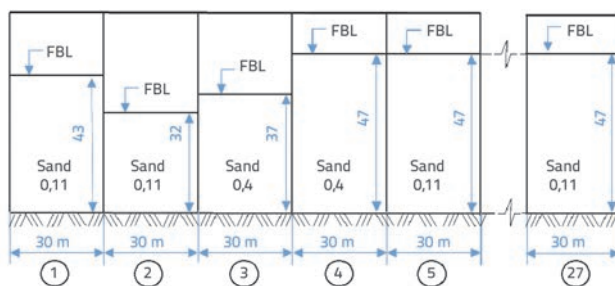


Figure 4. A fragment from construction scheme of test section

The following four devices were used to determine the FBL strength on the test section: dynamic – FWD Dynatest 8000 (FWD), LWD Prima 100 (LWD), ZORN ZSG 02 (ZORN), and static–

Table 1. Comparison of normative and actual physical and mechanical properties of subgrade and FBL

Layer of road structure	Values of deflection modulus [MPa]		Coefficient of filtration [m/day]		Total passing through 0.063 mm sieve [%]		Total passing through 2 mm sieve [%]	
	standard	actual	standard	actual	standard	actual	standard	actual
FBL	120	113.4 - 167.1	≥ 2	4.0 - 15.0	≤ 7	0.6 - 1.1	28 - 80	73.3 - 82
Subgrade	> 45	> 100			-			

Table 2. Statistical characteristics of deflection modulus

Values of deflection modulus	Measurement devices of deflection modulus			
	SB	LWD	ZORN	FWD
Maximal value [MPa]	167.1	139.3	50.8	236.7
Minimal value [MPa]	113.4	49.3	28.5	151.0
Mean value \bar{X} [MPa]	136.6	78.8	43.2	188.0
Standard deviation (SV) s [MPa]	15.4	16.2	5.3	22.8
Variation coefficient (CoV) [%]	11.3	20.5	12.3	12.1

static beam Strassentest (SB). Measurements were carried out using the same scheme (the measuring point varies ± 0.5 m), under the same weather conditions in August (average air temperature of 18°C, without precipitation).

The static deflection modulus E_{v2} was obtained from SB measurements, while the dynamic deflection moduli E_{vd} were obtained from the measurements conducted via three dynamic measuring devices. The deflection modulus measured at the test section for subgrade revealed that the deflection modulus is higher than 45 MPa at all measuring points (Table 1). Therefore, the subgrade strength is sufficient and it will likely have no effect on FBL deformations. The 0/11 sand fraction (at 25 sub-sections) and 0/4 sand fraction (at sub-sections 3 and 4) were used for FBL construction.

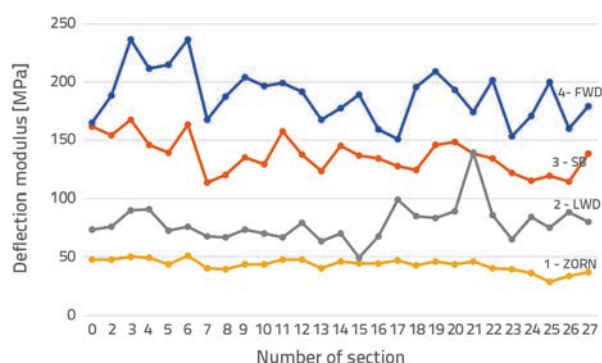
The FBL thickness at the first subsection, second subsection, and third subsection is 43 cm, 32 cm, and 37 cm, respectively, while the FBL thickness for subsections from 4 to 27 is 47 cm. The FBL filtration coefficient values at sub-sections 3 and 4 varied from 4.0 to 4.3 m/day (the recommended ones are at least 2 m/day). At all the other sub-sections, the filtration coefficient values ranged from 11.7 to 15.0 m/day. Values for FBL mineral mixture passing through a 2 mm sieve ranged from 73.3 to 82.0 % (the recommended range is 28–80 %) of the mixture weight. The values of material passing through a 0.063 mm sieve ranged from 0.6 to 1.1 % of the mixture (the recommended limit is up to 7 %). Different values of FBL deflection modulus may have been influenced not only by the devices, but also by various physical indicators: layer thickness, filtration coefficient, and gradation.

4. Results and discussion

4.1. Interaction between FBL physical indicators and deflection modulus

The measurement results for the FBL deflection modulus show that the readings obtained by static and dynamic devices at 27

sub-sections are substantially different and that they vary to a great extent (Figure 5).

**Figure 5. Deflection modulus of FBL measured by all devices: 1 – ZORN, 2 – LWD, 3 – SB, 4 – FWD**

The arithmetic average and dispersion characteristics (standard deviation and coefficient of variation) of the base position were calculated to enable comparison of different data sets (Table 2). The difference of arithmetic averages of deformation modulus, obtained by SB and dynamic devices (LWD, ZORN and FWD), was calculated using the following eq. (4):

$$\Delta E = \frac{\bar{E}_{v2} - \bar{E}_{vd}}{\bar{E}_{v2}} \cdot 100 \% \quad (4)$$

where:

\bar{E}_{v2} - is the arithmetic average of the SB-measured deflection modulus

\bar{E}_{vd} - is the arithmetic average of the deflection modulus measured by the dynamic device.

FWD, ZORN and SB showed similar stability according to variation coefficient values. The most unstable values were obtained using the LWD.

The analysis of results shows that the deflection-modulus numerical values, compared to the SB values, are different. LWD values (E_{LWD}) are about 42.3 % lower than the SB values (E_{SB}), when an average numeric value of deflection modulus was measured. ZORN (E_{ZORN}) values are about 68.4 % lower than the SB-measured values, and the FWD (E_{FWD}) values increased by about 37.6 %. According to the results, it can be seen that the lowest averages and lowest dispersion results were obtained using the ZORN device.

The impact of FBL physical indicators (layer thickness, filtration coefficient, percent passing through the 0.063 mm sieve, and total retained on the 2 mm sieve) on deflection modulus was determined using the correlation – regression analysis (Figure 6–9).

The SB and ZORN deflection modulus value decreases with an increase in the FBL layer thickness (Figures 6a and 8a). However, the LWD and FWD showed the opposite result: the values of deflection modulus increase with an increase in the FBL layer thickness (Figures 7.a and 9.a). It was determined that the deflection modulus values decrease as the filtration coefficient goes up (Figures 6.b–9.b). The values of deflection modulus decrease with an increase in the percent passing through the 0.063 mm sieve (Figures 6.c–9.c). This means that the finer the passing fraction (smaller than 0.063 mm), the weaker the primer (NEJASNO). The values of deflection

modulus decrease with an increase in the percent retained on the 2 mm sieve (Figures 6.d–9.d).

To validate the statistical hypothesis about the equality of correlation coefficient values to zero, the Student’s t-test was made and its statistic t was calculated as follows [34]:

$$t_{t-\alpha, m-2} = r \cdot \sqrt{\frac{m-2}{1-r^2}} \tag{5}$$

where: m is the number of criteria (m = 27) and r is the pairwise correlation coefficient.

The lowest value of the pairwise correlation coefficient r_{min} can be calculated by rearranging equation (5) as follows:

$$r_{min} = \frac{t_{\alpha, \nu}}{\sqrt{m-2 + t_{\alpha, \nu}^2}} \tag{6}$$

For the test section consisting of 27 sub-sections, with the significance level $\alpha = 0.05$ and the degree of freedom $\nu = 27 - 1 = 26$, the Student’s criterion critical value is $t_{\alpha, \nu} = 2.06$. The minimum correlation coefficient value r_{min} , calculated using the Eq6 formula and amounting to 0.381, allows the authors to conclude that the values are correlated.

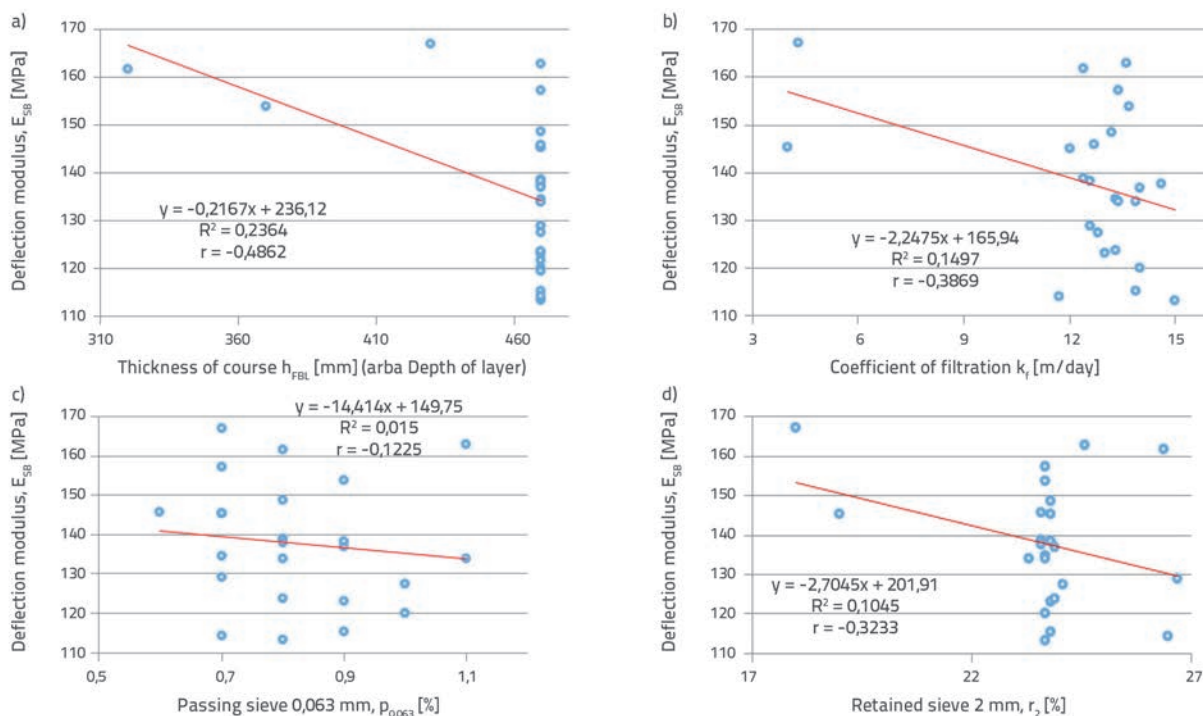


Figure 6. Impact of FBL physical indicators on deflection modulus E_{sg} , measured by SB: a) layer thickness; b) filtration coefficient; c) percent passing through 0.063 mm sieve; d) percent retained on 2 mm sieve

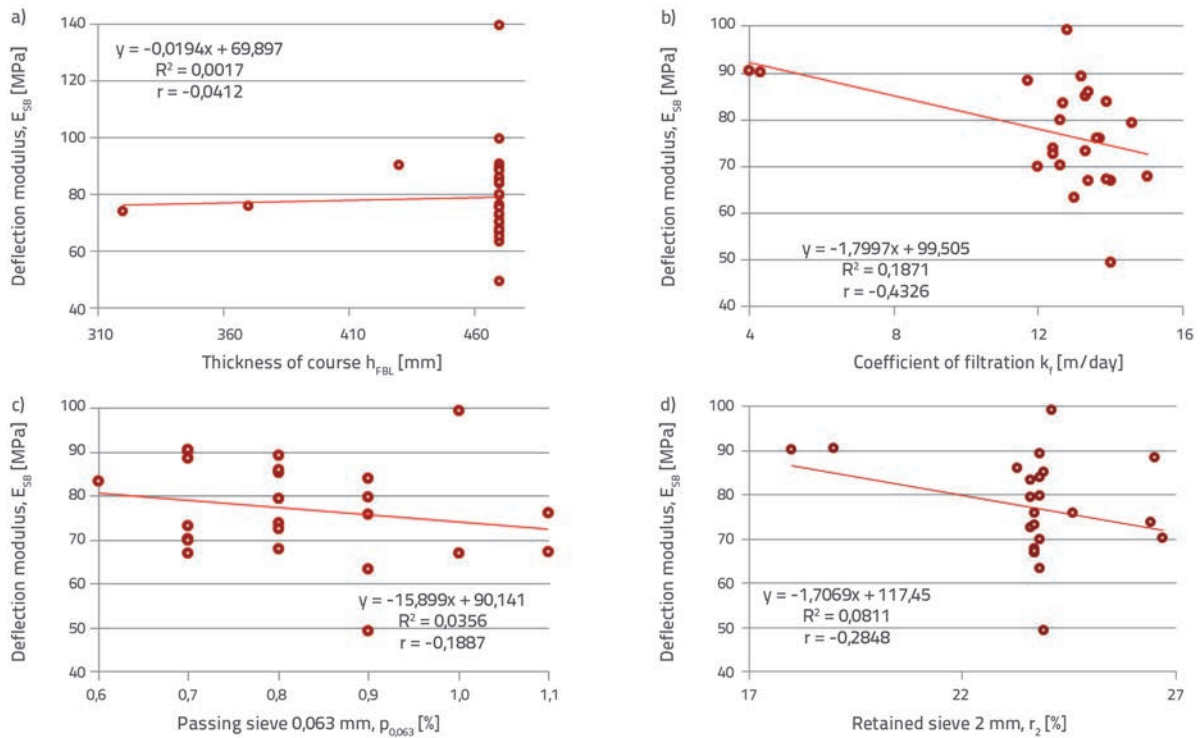


Figure 7. Impact of FBL physical indicators on deflection modulus E_{LWD} , measured by LWD: a) layer thickness; b) filtration coefficient; c) percent passing through 0.063 mm sieve; d) percent retained on 2 mm sieve

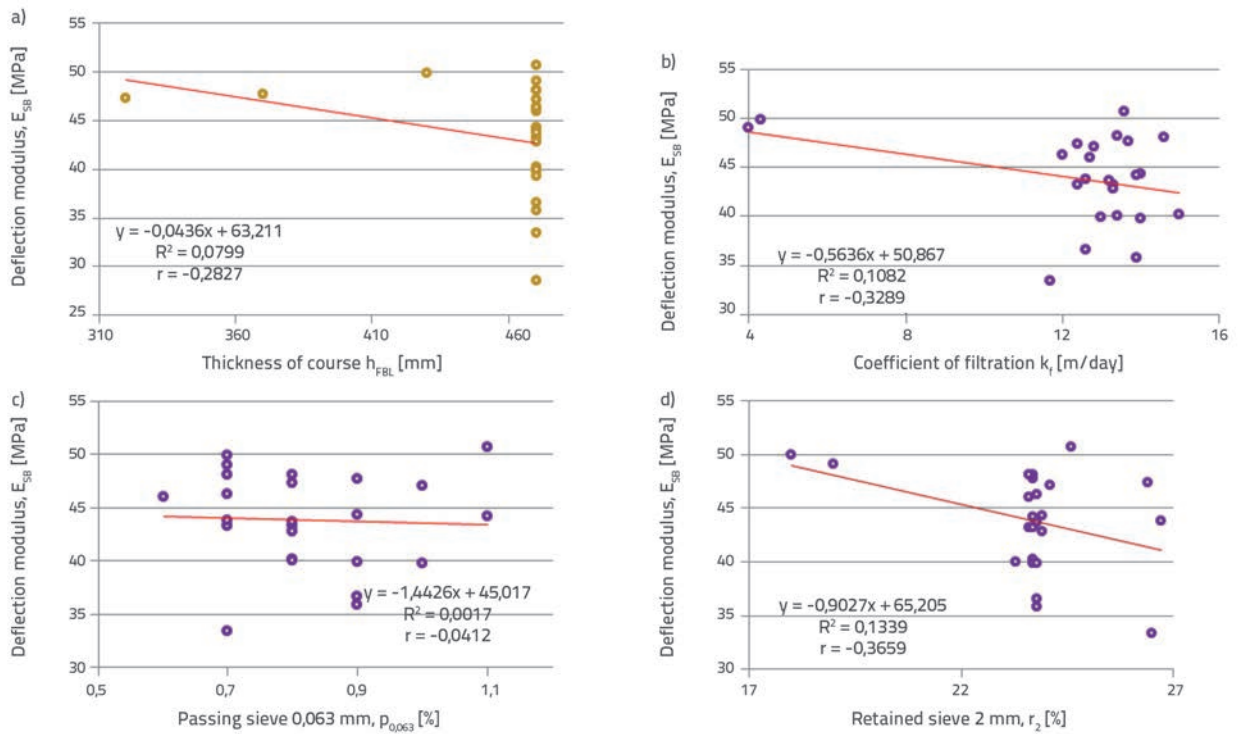


Figure 8. Dependence of the deflection modulus E_{ZORN} of FBL, measured by the ZORN dynamic device, on FBL physical indicators: a) layer thickness; b) filtration coefficient; c) percent passing through 0.063 mm sieve; d) percent retained on 2 mm sieve

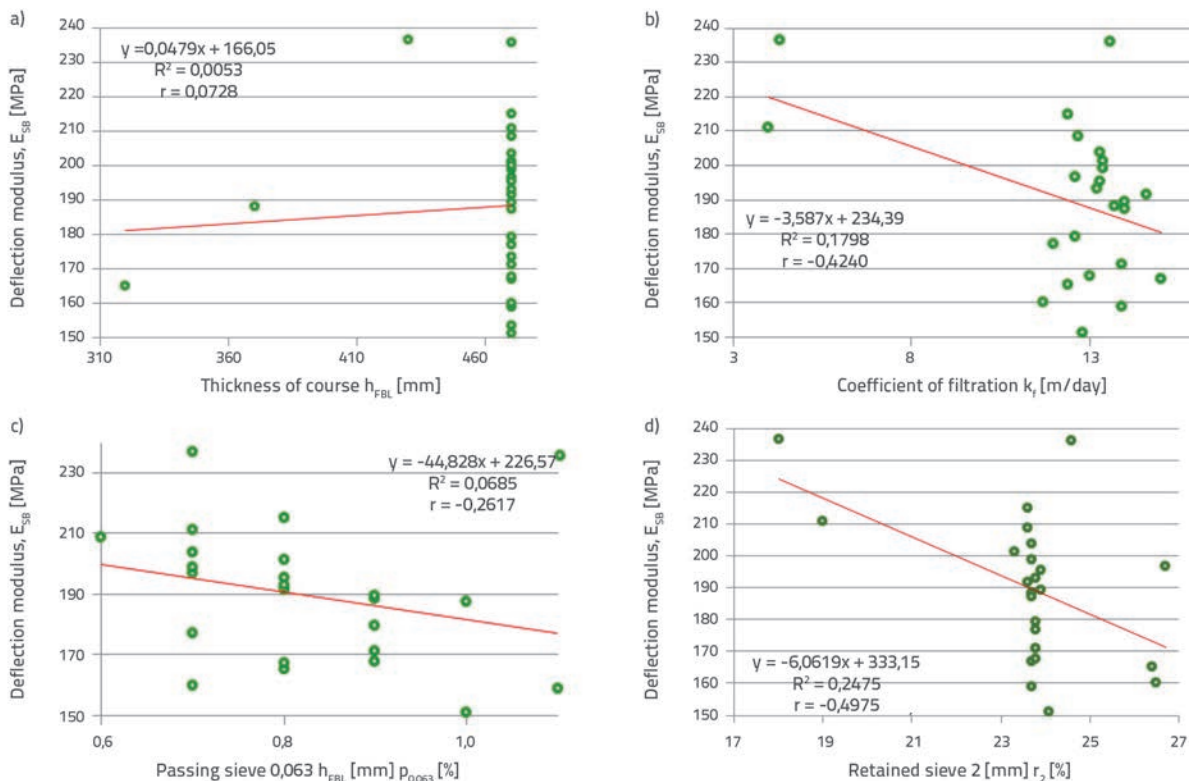


Figure 9. Impact of FBL physical indicators on deflection modulus E_{sB} measured by FWD: a) layer thickness; b) filtration coefficient; c) percent passing through 0.063 mm sieve; d) percent retained on 2 mm sieve

Table 3. Correlation coefficients between deflection modulus, measured by different devices, and FBL physical properties

Device	Correlation coefficients r of FBL physical properties			
	h_{FBL}	k_f	$p_{0.063}$	r_2
SB	-0.486	-0.387	-0.123	0.323
LWD	0.041	-0.433	-0.189	0.285
ZORN	-0.283	-0.329	-0.041	0.366
FWD	0.073	-0.424	-0.262	0.498

The h_{FBL} and k_f (Table 3) show the impact on the deformation modulus measured by the SB. Only k_f impacted the deflection modulus measured by the LWD. There was no interaction between physical indicators and deflection modulus measured by the ZORN device. The FWD deflection modulus depended on k_f and r_2 only.

These data show that the correlation between the deflection modulus, measured by different devices, and physical indicators of the test section FBL is not strong. The correlation would possibly be stronger if physical FBL indicators were adjusted in a larger interval.

4.2. Comparative analysis of readings shown by different devices

A regression model was used to determine the interaction between the readings of dynamic and static devices. The model was based on the assumption that if the SB reading is equal to 0 the readings of dynamic devices will also be equal to 0. The linear equation is as follows:

$$y = a_0 \cdot x \tag{7}$$

where a_0 is free member of the regression equation and x is variable, i.e. dynamic device reading.

After experimental data processing, the regression equations and their determination coefficients R^2 (Figure 10) were obtained. It was established that the readings of different devices are correlated.

Correction coefficients determined between different devices are constant. Correction coefficients must be used to obtain the SB imposed deflection modulus value (Table 4).

The SB reading was obtained by multiplying certain dynamic device readings by correction coefficient.

Table 4. Values of correction coefficients

SB deflection modulus	Correction coefficient		
	FWD	LWD	ZORN
E_{SB}	$0.72 \cdot E_{FWD}$	$1.67 \cdot E_{LWD}$	$3.15 \cdot E_{ZORN}$

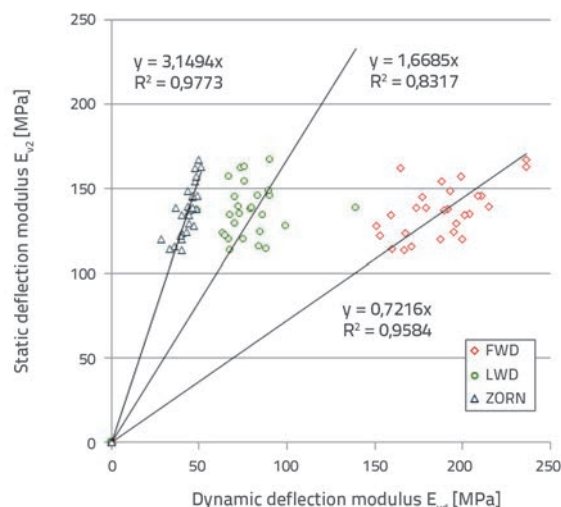


Figure 10 Regression model for recalculation of dynamic deflection modulus E_{vd} obtained from FWD, LWD, and ZORN data, into static deflection modulus E_{v2}

Correction coefficients were determined for each dynamic device based on the regression model. To obtain the SB deflection modulus value, the E_{FWD} , E_{LWD} and E_{ZORN} values must be multiplied by 0.72, 1.67, and 3.15, respectively (Table 4). This does not correspond to the dependency presented in Figure 3a. The deflection modulus measured by any of the dynamic devices (LWD, ZORN, FWD) has to be compared with normative specifications presented in SB. The correction coefficient values

proposed in the paper can be used to obtain the SB readings and to assess the FBL strength.

5. Conclusion

Average FBL deflection moduli values, measured by different devices at the test section with 27 different sub-sections, are fundamentally different and exhibit certain dispersion. The average LWD and ZORN deflection moduli values, i.e. 42.3 % and 68.4 %, were lower than the average values measured by the SB. The average FWD value was by 37.6 % higher than the average deflection modulus values measured by SB. The standard deviation (SD) values showed that the most stable readings (with lowest dispersion) were obtained with the ZORN device: SD = 5.3 MPa. SB and LWD were less stable with SD = 15.4 MPa and SD = 16.2 MPa, respectively, while variations were the greatest for the FWD readings (SD = 22.8 MPa). The coefficient of variation (CoV) increased as follows: SB (CoV = 11.3 %); FWD (CoV = 12.1 %); ZORN (CoV = 12.3 %), and LWD (CoV = 20.5 %).

The impact of FBL physical parameters on deflection modulus was established by the correlation–regression analysis. The layer thickness h_{FBL} affected only the modulus measured by the SB. The deflection modulus was affected by the filtration coefficient measured with the SB, LWD, and FWD devices. The percent passing through the 0.063 mm sieve had no impact on the readings of any devices. The total retained on the 2 mm sieve influenced only the readings of the FWD device.

The regression model was used to determine correction coefficients for each device. In order to get the SB deflection modulus values, the E_{FWD} , E_{LWD} and E_{ZORN} values must be multiplied by 0.72, 1.67, and 3.15, respectively. For other FBL physical properties, these coefficients have to be adjusted as appropriate.

REFERENCES

- [1] Zhang, X., Presler, W., Li, L., Jones, D., Odgers, B.: Use of wicking fabric to help prevent Frost boils in Alaskan pavements, Journal of Materials in Civil Engineering, 26 (2014) 4, pp. 728-740, [https://doi.org/10.1061/\(ASCE\)MT.1943-5533.0000828](https://doi.org/10.1061/(ASCE)MT.1943-5533.0000828)
- [2] Juknevičiūtė-Žilinskienė, L., Laurinavičius, A.: Evaluation of possibilities for the climatic distribution of regions from the point of view of road construction, The Baltic Journal of Road and Bridge Engineering, 10 (2015) 3, pp. 262-268, <https://doi.org/10.3846/bjrbe.2015.33>
- [3] Remišova, E., Decky, M., Podolka, L., Kovač, M., Vondračková, T., Bartuška, L.: Frost Index from Aspect of Design of Pavement Construction in Slovakia, Procedia Earth and Planetary Science, 15 (2015), pp. 3-10, <https://doi.org/10.1016/j.proeps.2015.08.002>
- [4] Riehma, M., Gustavsson, T., Bogren, J., Jansson, P.: Ice Formation Detection on Road Surfaces Using Infrared Thermometry, Cold Regions Science and Technology, 83 (2012) 34, pp. 71-76, <http://dx.doi.org/10.1016/j.coldregions.2012.06.004>
- [5] Monnet, J., Boutonnier, L.: Calibration of an unsaturated air-water-soil model, Archives of Civil and Mechanical Engineering, 12 (2012), pp. 493-499, <https://doi.org/10.1016/j.acme.2012.07.001>
- [6] Vaičiukynas, V., Vaikasas, S., Sivilevičius, H., Grinys, A.: The impact of agriculture drainage reconstruction on ground water recession close to the subgrade, The Baltic Journal of Road and Bridge Engineering, 10 (2015) 3, pp. 230-238, <https://doi.org/10.3846/bjrbe.2015.29>

- [7] Pospisil, K., Zednik, P., Stryk, J.: Relationship between deformation moduli obtained using light falling weight deflectometer and static plate test on various types of soil, *The Baltic Journal of Road and Bridge Engineering*, 9 (2014) 4, pp. 251-259, <https://doi.org/10.3846/bjrbe.2014.31>
- [8] Mateos, A., Soares, J.B.: Characterization of stiffness of unbound materials for pavement design: do we follow the right approach?, *Journal of Transportation Engineering*, 140 (2014) 4, [https://doi.org/10.1061/\(ASCE\)TE.1943-5436.0000645](https://doi.org/10.1061/(ASCE)TE.1943-5436.0000645)
- [9] Zhou, C., Huang, B., Drumm, E., Shu, X., Dong, Q., Udeh, S.: Soil resilient modulus regressed from physical properties and influence of seasonal variation on asphalt pavement performance, *Journal of Transportation Engineering*, 141 (2015) 1, [https://doi.org/10.1061/\(ASCE\)TE.1943-5436.0000727](https://doi.org/10.1061/(ASCE)TE.1943-5436.0000727)
- [10] Abu-Farsakh, M.Y., Mehrotra, A., Mohammad, L., Gaspard, K.: Incorporating the effect of moisture variation on resilient modulus for unaturated fine-grained subgrade soils, *Transport Research Record: Journal of the Transportation Research Board*, 2510 (2015), pp. 44-55, <https://doi.org/10.3141/2510-06>
- [11] Bazi, G., Briggs, R., Saboundjian, S., Ullidtz, P.: Seasonal effects on a low-volume road flexible pavement, *Transport Research Record, Journal of the Transportation Research Board*, 2510 (2015), pp. 81-89, <https://doi.org/10.3141/2510-010>
- [12] Rajaei, P., Baladi, G.Y.: Frost depth general prediction model, *Transport Research Record: Journal of the Transportation Research Board*, 2510 (2015), pp. 74-80, <https://doi.org/10.3141/2510-09>
- [13] Salour, F., Erlingsson, S., Zapata, C.E.: Model for seasonal variation of resilient modulus in silty sand subgrade soil, *Transport Research Record: Journal of the Transportation Research Board*, 2510 (2015), pp. 65-73, <https://doi.org/10.3141/2510-08>
- [14] Titi, H.H., English, R., Faheem, A.: Resilient modulus of fine-grained soils for mechanistic - empirical pavement design, *Transport Research Record: Journal of the Transportation Research Board*, 2510 (2015), pp. 24-35, <https://doi.org/10.3141/2510-04>
- [15] Vennapusa, P.K.R., White, D.J., Siekmeier, J., Embacher, R.A.: In situ mechanistic characterisations of granular pavement foundation layers, *International Journal of Pavement Engineering*, 13(1), pp. 52-67, 2012. <https://doi.org/10.1080/10298436.2011.564281>
- [16] Nam, B.H., Stokoe, K.H.: Improved Rolling Dynamic Deflectometer for continuous pavement deflection measurements, *Journal of Testing and Evaluation*, 42 (2014) 2, pp. 312-327, <https://doi.org/10.1520/JTE20120262>
- [17] Elhakim, A.F., Elbaz, K., Amer, M.I.: The use of light weight deflectometer for in situ evaluation of sand degree of compaction, *HBRC Journal*, 10 (2014), pp. 298-307, <https://doi.org/10.1016/j.hbrj.2013.12.003>
- [18] Chai, G.W., van Staden, R., Loo, Y.C.: In situ assessment of pavement subgrade using Falling Weight Deflectometer, *Journal of Testing and Evaluation*, 43 (2015) 1, pp. 140-148, <https://doi.org/10.1520/JTE20130149>. ISSN 0090-3973
- [19] Subgrade installation ST 188710638.06: 2004, The rules for construction, the Lithuanian Road Administration, Vilnius, 2004.
- [20] Bilodeau, J.P., Doré, G.: Direct estimation of vertical strain at the top of the subgrade soil from interpretation of falling weight deflectometer deflection basins, *Canadian Journal of Civil Engineering*, 41 (2014) 5, pp. 403-408, <https://doi.org/10.1139/cjce-2013-0128>
- [21] Bilodeau, J.P., Doré, G.: Stress distribution experienced under a portable light-weight deflectometer loading plate, *International Journal of Pavement Engineering*, 15 (2014) 6, pp. 564-575, <https://doi.org/10.1080/10298436.2013.772612>
- [22] Kim, J.R., Kang, H.B., Kim, D., Park, D.S., Kim, W. J.: Evaluation of in situ modulus of compacted subgrades using portable falling weight deflectometer and plate-bearing load test, *Journal of Materials in Civil Engineering*, 19 (2007) 6, pp. 492-499, [https://doi.org/10.1061/\(ASCE\)0899-1561\(2007\)19:6\(492\)](https://doi.org/10.1061/(ASCE)0899-1561(2007)19:6(492))
- [23] Ullidtz, P.: *Modeling Flexible Pavement Response and Performance*, Denmark, 1998, 205 p.
- [24] Kavussi, A., Rafiei, K., Yasrobi, S.: Evaluation of PFWD as potential quality control tool of pavement layers, *Journal of Civil Engineering and Management*, 16 (2010) 1, pp. 123-129, <https://doi.org/10.3846/jcem.2010.11>
- [25] Tompai, Z.: Conversion between static and dynamic load bearing capacity moduli and introduction of dynamic Target Values, *Civil Engineering*, 52 (2008) 2, pp. 97-102, <https://doi.org/10.3311/pp.ci.2008-2.06>
- [26] Sulewska, M.J.: The application of the modern method of embankment compaction control, *Journal of Civil Engineering and Management*, X, pp. 45-50, 2004. ISSN 1392-3730
- [27] Sulewska, M.J.: The control of soil compaction degree by means of LFWD, *The Baltic Journal of Road and Bridge Engineering*, 7 (2012) 1, pp. 36-41, <https://doi.org/10.3846/bjrbe.2012.05>
- [28] Bertulienė, L.: Assessment, research and use of methods for determining the strength of base courses of road pavement structure, *The Baltic Journal of Road and Bridge Engineering*, 7 (2012) 3, pp. 228-236, <https://doi.org/10.3846/bjrbe.2012.30>
- [29] Janulevičius, J., Čygas, D., Giniotis, V., Aavik, A.: Assumptions to road pavement testing by non-destructive means, *The Baltic Journal of Road and Bridge Engineering*, 8 (2013) 4, pp. 227-231, <https://doi.org/10.3846/bjrbe.2013.29>
- [30] Soils for road construction. Testing methods. Plate load test, LST 1360.5:1995, Lithuanian Standardization Department, Vilnius, 1995.
- [31] Čygas, D., Laurinavičius, A., Paliukaitė, M., Motiejūnas, A., Žiliūtė, L., Vaitkus, A.: Monitoring the mechanical and structural behavior of the pavement structure using electronic sensors, *Computer - Aided Civil and Infrastructure Engineering*, 30 (2015) 4, pp. 317-328, <https://doi.org/10.1111/mice.12104>
- [32] Standardized design rules for the road pavement structures KPT SDK 07, The Lithuanian Road Administration, Vilnius, 2007.
- [33] Road pavement layers without binders installation rules JT SBR 07, The Lithuanian Road Administration, Vilnius, 2007.
- [34] Podvezko, V., Sivilevičius, H.: The use of AHP and rank correlation methods for determining the significance of the interaction between the elements of a transport system having a strong influence on traffic safety, *Transport*, 28 (2013) 4, pp. 389-403, <https://doi.org/10.3846/16484142.2013.86>